



Effective Application of *Jatropha Curcas* Husk Activated ZnCl₂ for Adsorption of Methylene Blue: Isotherm, Kinetics and Development of Empirical Model

Kiman Silas^{a,*}, Musa Y. Pudza^b, Habiba D. Mohammed^a

^aDepartment of Chemical Engineering, University of Maiduguri, Bama Road, PMB 1069 Maiduguri, Borno State, Nigeria

^bDepartment of Chemical and Environmental Engineering, Universiti Putra Malaysia, 43400 UPM Serdang, Selangor, Malaysia

ARTICLE INFO

Article history:

Received 14 December 2021

Received in revised form 24 March 2022

Accepted 29 March 2022

Available online 28 May 2022

ABSTRACT

Water conservation is critical for both the natural environment and human development however, there is wastewater generation, particularly in the production of pulp, printing, leather, plastic, dye, and textile mills. Large-scale industrial wastewater purification necessitates the employment of low-cost adsorbents to lower the cost of large-scale industrial wastewater treatment procedures. In this study, the husk of *Jatropha curcas* (JHC) was carbonized, activated, and impregnate with ZnCl₂ for use in batch tests to adsorb methylene blue (MB) from an aqueous solution. The effects of concentration, stirring speed, contact time, pH, and adsorbent dosage on adsorption isotherms and kinetics were examined. The Freundlich isotherm model accurately described the adsorption isotherm, while pseudo-second-order adequately fitted the kinetic data. The dye-loaded adsorbent could be regenerated by chemical regeneration after five desorption cycles. These findings suggested that JHC could be a good adsorbent for removing MB from wastewater and could help with industrial wastewater treatment.

1. Introduction

The discharge of colored wastewater/dye effluent into the aquatic environment because of the activities of various industries such as paper and pulp, printing, leather, plastic, textile, and dye, poses threats to humans, animals, and the environment [1]. Significant amounts of organic pollutants discharged by industry may be hazardous to flora and wildlife, lowering autotrophic organism photosynthesis substantially [2]. The textile dyeing industry produces and releases 280,000 tons of dyes into water streams each year across the world [3,4]. Dyes are organic molecules that are less biodegradable due to their complex aromatic molecular structure. Methylene blue (MB) is cationic [5], and it's widely used in cotton, textiles, wools, and colorants, with reports of material durability and ease of use [6,7]. MB can have various harmful effects on both humans and animals [8,9] due to its chemical properties which may lead to mutagenic and carcinogenic properties in a wide range of living beings [10]. Among the several dye removal

procedures available, including catalytic oxidation, electrochemical oxidation, biological therapy, coagulation/flocculation, ozonation, photocatalytic degradation, and sonocatalytic degradation, adsorption stands out as the most effective [1]. The adhesion of atoms, ions, gas, liquid, or dissolved solids to a surface is known as adsorption [11]. Other procedures have the disadvantages of creating toxic sludge, carcinogenic byproducts, costly equipment, and energy costs. Also, water treatment by adsorption may cost 5.0–200 USD m⁻³, whereas other technologies may cost twice as much [2]. It is a well-known technology to use Activated Carbon (AC) as an adsorbent in wastewater treatment [12-14]. When nonrenewable commercial AC-based for removing dyes is used, materials such as coal and petroleum coke are expensive consequently, agricultural biomass can be employed because of the advantages of eco-friendly and low-cost alternative resources [3,4]. JHC is a good source for the development of ACs in the adsorption process because it is cheap and is an agro-industrial solid waste [1,4,15]. Adsorption ability is a function of surface area,

* Corresponding author.; e-mail: silaskiman@gmail.com; Tel. +60108476412

and chemical activation adds to a larger surface area [16]. Zinc chloride ($ZnCl_2$) activation of JHC may create larger interspaces between carbon layers, resulting in porosity and increased surface area [4]. Jatropha curcas seed and press cake were tested for coagulative behaviors and wastewater treatment abilities in a previous study [17]. The surface response methodology (RSM) is a useful tool for deciphering the relationship between two or more input variables [18-19], and RSM has improved the experimental conditions of many chemical processes. Previously, Charola *et al.* [5] studied, the influential adsorption parameters (initial pH, adsorbent dosage, temperature, and initial concentration of MB by oil palm leaves (OPL) with the RSM technique. Mohebali *et al.* [20] reported the adsorption isotherm and kinetic models MB adsorption process onto modified celery residue but no optimization has been reported.

The objective of this study is to utilize the agro-based waste (JHC) impregnated $ZnCl_2/AC$ and used in the removal of MB. The effects of operational parameters, equilibrium isotherm, and kinetics of MB removal by JHC were studied. Furthermore, the reusability of the adsorbent was investigated in five adsorption/desorption cycles. The analysis of variance (ANOVA) based on RSM was used to investigate the influence of adsorption parameters of JHC towards the MB adsorption while the interactive effects of these operating parameters on the adsorption process were evaluated and an empirical correlation is established which describes the adsorption efficiency.

2. Results and Discussion

2.1. Adsorption Process

The adsorption capacity and removal percent are calculated by using following Equations [21, 22]:

$$qe = \frac{(Co - Cf)v}{M} \quad (1)$$

$$\% \text{ Removal} = \frac{Co - Cf}{Co} \times 100 \quad (2)$$

Where, q_e is the adsorption capacity measured in mg/g, M is the mass of the adsorbent applied in the study (g), V is the volume of the dye solution measured in L, C_o is the initial concentration of dye sample measured in mg/L, C_f is the equilibrium of the concentration of dye in sample measured in mg/L.

2.1.1 Effect of operation parameters

As shown in Fig. 1(a), by raising the concentration, amount of adsorbent, the amount adsorbed increased. The adsorption was fast at first, but it gradually slowed as the contact duration increased, and the adsorption stabilized once equilibrium was attained at about 80 minutes. The availability of many unoccupied surface sites was responsible for the early rapid adsorption of MB. As a result of the increased initial dye

concentration, the driving force for mass transfer improved.

The investigation results of the effect of dosage are presented in Fig. 1(b). The adsorbent dosage is an important parameter that influences the adsorption capacity of the adsorbent. The effects of JHC dose on the adsorption of MB were investigated by varying the adsorbent dose from 1-5 g at constant stirring speed (140 rpm) and concentration (50 mg/L).

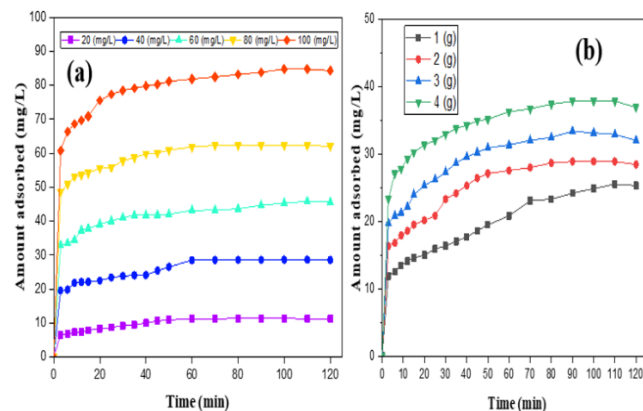


Figure 1. (a) Effect of concentration (b) Effect of dosage

The amount of MB adsorbed was initially high, but it gradually decreased over time until it reached equilibrium. This phenomenon occurred because the rate of adsorption is higher at first since there are more active sites available for reaction however the adsorption decreases over time due to pore site blockage, in agreement with other research work [11]. The JHC adsorbent reached maximum adsorption in 60 minutes for concentrations of 20 - 40 mg/L, while it took longer to reach equilibrium in 60 mg/L (80 min), 80 mg/L, and 100 mg/L (100 min) concentrations indicating that the higher the concentration, the higher the equilibrium due to possible pore blockage by MB whole molecules increases with increased concentration. The effect of stirring time in Fig. 2(a) was studied when the size of JHC of 0.5 mm, the concentration of 50 mg/L, dose of 5g, and pH of 13 were used, the equilibrium time for JHC was found to be 40 min (60 and 80 rpm) and 50 min (100, 120 and 140 rpm) respectively.

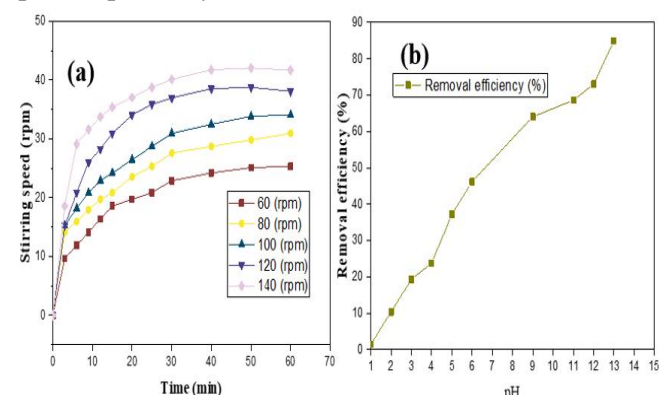


Figure 2. (a) the effect of stirring speed (b) pH of aqueous solution

Fig. 2 (b) shows that the pH of the aqueous solution has a considerable impact on the JHC's absorption capacity. The surface binding-sites and ionization process of the MB molecule are influenced by the adsorbent's molecules therefore, the pH values can be explained in terms of electrostatic interactions between the adsorbent and the adsorbate. Fig. 2 (b) suggests that as the pH is increased, the amount adsorbed increases, a similar plot can be found in the literature [23].

2.2. Characterization Results

The surface area plays an important role in the adsorption process where there is available surface area for the adsorption to take place. Table 1 shows the BET surface area results of the ZnCl₂/JHC adsorbent before and after adsorption.

Table 1. BET surface area results of the ZnCl₂/JHC adsorbent

Adsorbent	Surface area (m ² /g)	Pore volume (cm ³ /g)	Pore size (Å)
ZnCl ₂ /JHC Before adsorption	24.8255	0.003602	50.444
ZnCl ₂ /JHC After adsorption	2.6258	0.000028	49.667

When compared to the adsorbent before adsorption, the surface area of the adsorbent is drastically reduced after adsorption. This is due to adsorbate pore obstruction, which causes surface area saturation [18,24]. Fig. 3(a) showed a lot of pores, which are essential for successful adsorption. The SEM picture (Fig. 3b) was loaded by MB adsorption when the JHC pores were partially occupied, changing the adsorbent into irregular structures, indicating that the MB adsorption was strong.

Fig. 3(c) shows the FTIR spectra used to investigate the functional groups present on the surface area. The adsorbent is bound with functional groups. The functional groups present on the JHC adsorbent before and after adsorption were visible in the FTIR spectrum. The presence of phenolic groups on both adsorbents was revealed by stretching bands at 1035-1044 cm⁻¹, which is attributable to the presence of lignin structure in JHC [2]. C-H is responsible for the stretching at 2832 cm⁻¹ [17]. A broadband formed at 3382 cm⁻¹ on the JHC adsorbent before adsorption, which is attributed to the vibration of hydroxyl groups (O-H) [2,17], but this band did not appear on the JHC adsorbent after adsorption because of MB adsorption on the adsorbent.

After MB adsorption, JHC shows stretching at 1422 cm⁻¹, which is attributed to MB [11]. Changes in the intensity of absorbing groups caused spectral shifts, widening, and extinction of some bands. Furthermore, adsorption was discovered to occur due to complexation, electrostatic attraction between the JHC adsorbent's

surface and the adsorbate, or hydrogen bonding [2]. Figure 4 shows a void peak in amorphous systems like activated carbon.

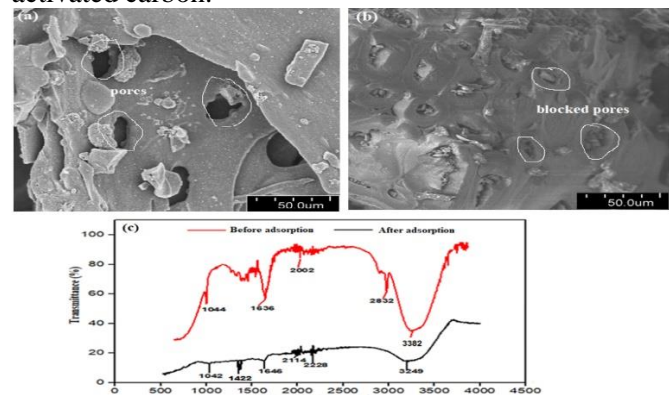


Figure 3. SEM images of (A) JHC before MB adsorption and (B) JHC after MB adsorption (c) FTIR spectra display of the adsorbent.

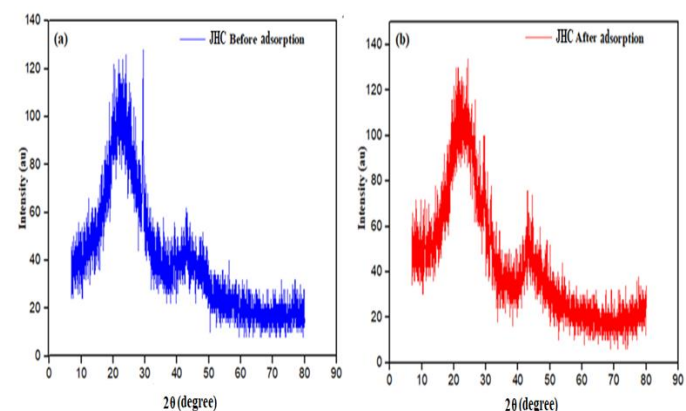


Figure 4. XRD pattern of JHC (a) before and (b) after adsorption

Fig. 4(a) shows JHC's XRD patterns, which show diffraction peaks at around 24.4°, 30.1°, 44.6°, and 46.4°, corresponding to the 220, 022, 020, and 202 planes. These peaks imply a thin amorphous layer on the JHC's surface, which could be owing to the irregular distribution of COOH groups on the JHC's surface, while other peaks could be due to incomplete carbonization. The peak intensities in Fig. 4(b) are essentially the same as those in Fig. 4(a), however there are several peaks around 43.4° and 48.1°. The number of XRD patterns as well as the peak intensity increased which suggested that the MB dyes was adsorbed on the surface of JHC adsorbent. Moreover, the peaks at 24.4 and 43.4 ° are ascribed to ZnCl₂ [2].

2.3. Adsorption Isotherms

Adsorption isotherms accurately reflect the interaction of the adsorbate with the adsorbent and aid in maximizing the adsorbent's utilization. According to the Langmuir isotherm, the intermolecular interactions between the adsorbing molecules are negligible, and

adsorption ceases when the surface sites on the adsorbent are entirely occupied [2]. Linear representation of Langmuir's isotherm is [25]:

$$q_e = \frac{(q_m K_L C_e)}{(1 + K_L C_e)} \quad (3)$$

Where, q_e denotes the adsorption of equilibrium capacity measured in mg/g, q_m denotes the maximum adsorption capacity required to form a monolayer on the surface of adsorbent measured in mg/g, and K_L denotes the Langmuir constant measured in L/g. The linearized form of Langmuir equation is:

$$\frac{C_e}{q_e} = \frac{1}{q_m K_L} + \frac{C_e}{q_m} \quad (4)$$

Where, q_m and K_L could be determined from the slope and intercept of linearized equation plot

$\frac{C_e}{q_e}$ against C_e [25]. The essential characteristics of

Langmuir dimensionless constant is referred to separation factor or equilibrium parameter (R_L) and it is defined as [11]:

$$R_L = \frac{1}{1 + K_L \cdot C_0} \quad (5)$$

Langmuir isotherm suitability could be unfavorable ($R_L > 1$) or favorable ($0 < R_L < 1$) [26,27].

The Freundlich adsorption isotherm defines heterogeneous systems which interact between the adsorbed molecules and expresses the exponential distribution of active sites with their energies, Freundlich isotherm is as follow [2, 25]:

$$q_e = k_f C_e^{1/n} \quad (6)$$

Where, k_f is Freundlich constant, $1/n$ is the heterogeneity factor indicating adsorption capacity. The linearized form Freundlich isotherm is:

$$\log q_e = \log k_f + 1/n \log C_e \quad (7)$$

Where, k_f incorporates the factors that affect the adsorption capacity and n affects the intensity of adsorption. A high value of k_f (slope) means a higher capability for adsorption and high value of n (intercept) means that good adsorption occurred over the entire studied range of concentrations however, a small value of n indicates that adsorption is good at high concentrations but less at lower concentrations [2].

Fig. 5(a) shows the Freundlich and Langmuir isotherms. The isotherm's applicability is demonstrated by the correlation coefficient (r^2), where the Langmuir sorption

isotherm explains monolayer adsorption on a homogeneous surface. The r^2 of 0.927 was obtained from the Langmuir isotherm plot, and the R_L value (1.1) was found to be out of the favorable range (see Table 2), indicating that the Langmuir model for the examined MB over JHC adsorbent is not suitable. From the Freundlich isotherm (Fig. 5b), the intensity of adsorption can be established from the slope ($1/n$) and the intensity of adsorption become more heterogeneous when its value got closer to zero. When the exponent n is more than 1 and the range of favorable adsorption is $1 < n < 10$ [25], the adsorption is considered favorable. The Freundlich isotherm indicate that adsorbate uptake happens on a heterogeneous surface with multilayer adsorption, and that greater K_f values indicate that adsorbate uptake is straightforward.

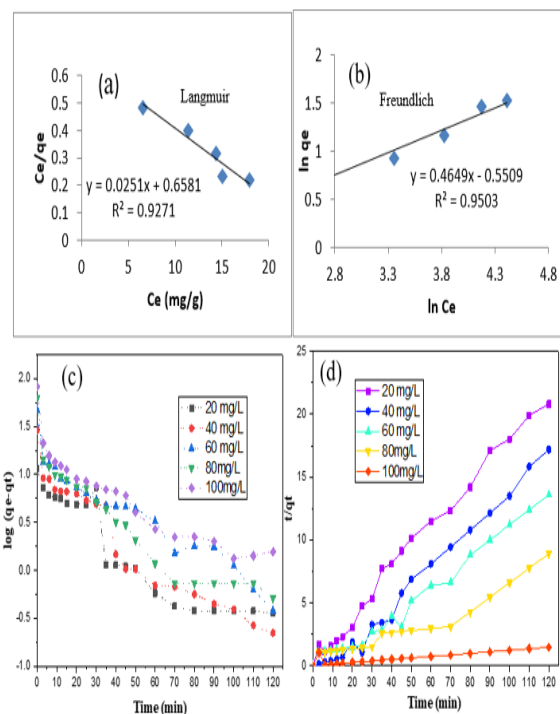


Figure 5. (a) Langmuir Isotherm and (b) Freundlich Isotherm (c) Initial dye concentration First order kinetics study (d) Initial dye concentration second order kinetics study.

The r^2 value of 0.9503 and the n value of 1.69 indicate the suitability of Freundlich isotherm to explain the adsorption process for the studied MB over JHC. Mohebali *et al.* [20] used celery residue modified with H_2SO_4 for methylene blue adsorption from aqueous solution in batch adsorption process and reported Freundlich isotherm model to best described the experimental data.

2.4. Adsorption Kinetics

The investigation of the mechanism of adsorption is performed with the Pseudo First-Order (PFO) and Pseudo Second-Order kinetic (PSO). The order rate model equation was first developed by Lagergren [28]. Fig. 5 (c and d) shows a linear form of

the model at varying MB concentration on JHC. The constant values of K_L was obtained by plotting a straight-line graph of $\log (q_e - q_t)$ against t . The regression coefficient of 0.9456 is obtained regarding concentration at 20 mg/l while 0.9063 for 100 mg/l.

The calculated value of adsorption capacity (q_{cal}) was obtained as 9.255 mg/g and 21.0546 mg/g at 100 mg/l. Based on the observed calculated and experimental

values, the adsorption of MB follows the Pseudo Second-Order kinetic model.

Pseudo-First-Order rate constant (k_1), Pseudo Second-Order kinetic rate constant (k_2), q_e , and q_{cal} were obtained from the slope and intercept of the graph in Fig. 5 (c and d). The results depict that pseudo-second order kinetic model presented a better correlation for the process of MB adsorption on JHC. Similar finding has been reported previously [6,20].

Table 2. Results of Langmuir and Freundlich isotherms

Model	n	1/n	K_F (mg ^{1-1/n} L ^{1/n} g ⁻¹)	R ²	q_m (mg/g)	K_L	R_L
Freundlich	1.78	0.682	0.096	0.9503	17.9	-	-
Langmuir	-	-	-	0.9271	12.2	0.05	1.1

2.5. Desorption Studies

The reusability and feasibility of employing JHC to remove MB from aqueous solution was tested in five adsorption/desorption cycles for resource and economic reasons. Chemical desorption of JHC with various HCl concentrations yielded low removal efficiencies, although the 0.1 mol/L concentration exhibited a better efficiency than the 0.001 mol/L values, which could be related to a change in adsorbent surface area in agreement with literature [7]. Overall, the MB removal was slightly

decreased from 89% to 86.7% after five cycles for 0.1 mol/L concentration which is <10% efficiency reduction indicating good performance. Liu et al. [8] reported the regeneration efficiency of less 70% for biochar loaded MB after three cycles. This adsorbent showed high stability thus, it has the potential of industrial application. The JHC adsorbent is regenerable, environmentally friendly, effective, and low-cost biomaterial for application in removal of MB from aqueous dye solutions and industrial effluents.

Table 3. ANOVA result

Source	Sum of		Mean	F	p-value	Remark
	Squares	df				
Model	1094.83	14	78.20	131.15	< 0.0001	a
A-pH	4.86	1	4.86	8.15	0.0020	a
B-Concentration	5.61	1	5.61	9.40	0.0018	a
C-Stirring Speed	4.86	1	4.86	8.15	0.0020	a
D-Dosage	3.38	1	3.38	5.66	0.0031	a
AB	147.62	1	147.62	247.57	< 0.0001	a
AC	165.12	1	165.12	276.92	< 0.0001	a
AD	40.96	1	40.96	68.69	< 0.0001	a
BC	299.29	1	299.29	501.93	< 0.0001	a

BD	0.30	1	0.30	0.51	0.4872	a
CD	264.06	1	264.06	442.85	< 0.0001	a
A ²	93.66	1	93.66	157.08	< 0.0001	a
B ²	13.84	1	13.84	23.22	0.0002	a
C ²	85.00	1	85.00	142.56	< 0.0001	a
D ²	10.22	1	10.22	17.14	0.0009	a
Residual	8.94	15	0.60			
Lack of Fit	7.74	10	0.77	3.23	0.1040	b
Pure Error	1.20	5	0.24			
Cor Total	1103.77	29				

a= significant, b= not significant

2.6. Analysis of Variance (ANOVA) and Regression Model Equation

The ANOVA table (Table 3) shows the assessment of the statistically significant of the CCD model also, the quadratic regression model indicated that the model was significant for the considered probability ($p = 0.05$). The Model F-value of 131.15 implies the model is significant. Values of "Prob > F" less than 0.0500 shows that the model terms are significant. In this case A, B, C, D, AB, AC, AD, BC, CD, A², B², C², D² are significant model terms. The "Lack of Fit F-value" of 3.23 implies the lack of fit is not significant. According to the ANOVA result, variable that influenced the adsorption process in hierarchy was the concentration, pH, stirring speed and dosage. The results were fitted to a linear model, leading to an empirical correlation that described the adsorption process.

The ANOVA result confirmed the adequacy of the empirical model which is represented in terms of coded factor as:

$$\text{MB Removal (\%)} = 50.4 + 0.45A - 0.48B + 0.45C + 0.37C - 3.04AB - 3.21AC + 1.6AD + 4.3BC + 0.1BD - 4CD - 1.8A^2 - 0.7B^2 - 1.7C^2 - 0.6D^2 \quad (8)$$

The goodness of fit of the model was also verified using r² between the experimental and model-predicted values of the response variables [18,29] (Fig. 6b). A high value of r² (0.9919) illustrates that the data variation was explained by the regression model. Further, the model can be used to know the MB removal percentage with variable concentration, pH, stirring speed, and dosage with respect to the adsorbent.

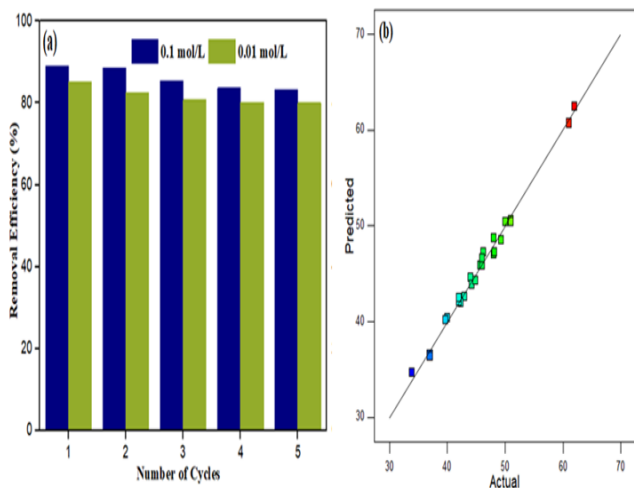


Figure 6. (a) Reusability of JHC for MB adsorption (b) Parity plot for the actual and predicted values of MB removal.

3. Experimental

3.1. Material

The chemicals methylene blue (chemical formula C₁₆H₁₈N₃SCl, molecular weight 319.85 g/mol), hydrochloric acid (HCl), and sodium hydroxide (NaOH) were purchased from Merck (Sdn Bhd) Malaysia. In deionized water, a stock solution of MB (1000 mg/L) was prepared and diluted to the appropriate concentrations (25–250 mg/L), and the pH of the solution was adjusted using adequate quantities of HCl or NaOH.

3.2. Adsorbent Preparation

The JHC was carbonized by crushing it first, then heating it for 1 hour at 800 °C at a rate of 5°C min⁻¹ under steady N₂ flow in a muffle furnace. To eliminate contaminants, the carbon precursor was washed with distilled water and oven-dried for 5 hours at 105 °C. For

1 hour on a stirrer, 2 L of hot water containing 450 g of ZnCl₂ was combined with the carbonized JHC (100rpm). The surplus ZnCl₂ was leached away for 24 h at 80°C in a hot 1.0M HCl solution, and it was repeatedly washed until a constant pH was achieved followed by 24 hours oven drying at 100°C.

3.3. Batch Adsorption Experiments

A closed Erlenmeyer flask of 250 mL was utilized as a batch system to evaluate the interaction between JHC and MB solution. The pH was adjusted to the desired value and various doses of JHC (1, 2, 3, and 4 g of adsorbent per 1 L of dye solution) were utilized. The temperature was kept constant at room temperature throughout the experiments, while various parameters such as contact time (3-120 min), pH (1-13), and initial dye concentrations (20, 40, 60, 80, and 100 mg/L) were investigated. The Erlenmeyer flasks containing the solution were mounted and agitated (60-140 rpm) in the illuminated refrigerated incubator shaker for improved mixing (Innova 4340, US). At the end of the equilibrium cycle, the suspensions were centrifuged at 140 rpm for 10 min, and then the suspension supernatant was filtered using a Millipore filter of 0.2 μm.

3.4. Desorption Experiments

In an Erlenmeyer flask covered with a rubber stopper, the MB loaded JHC was mixed with two different concentrations of HCl (0.1 and 0.001 mol/L) as the desorption solvent [1/3 (mg/mL) ratio] and shaken at 180 r/min and 25 °C for 24 hours. The resultant suspension was filtered and rinsed with deionized water after drying at 80 °C for 24 hours. On a UV-vis spectrophotometer (MAPADA UV-3300PC, Shanghai, China) with a 665 nm wavelength, the concentrations of MB were measured before and after adsorption.

3.5. Characterization

By adsorption and desorption of N₂ at 77 K, the Brunauer-Emmett-Teller (BET) method was used to calculate the Specific Surface Area (S_{BET}) and Total Pore Volume (V_p) using micrometrics (ASAP2020) for powders, which were outgassed for 4 hours at 200° C under inert gas flow. The functional groups of the adsorbent were also seen using Fourier transform infrared (FTIR) spectroscopy (Thermo Nicolet AES0200682), which uses a mercury-cadmium-telluride detector chilled with liquid nitrogen. A Field Emission Scanning Electron Microscope (FESEM) was used to examine the adsorbent morphology (Hitachi Co., Japan, Model No. S3400N). The component content of the adsorbent was investigated using an X-Ray Diffraction (XRD) X'Pert Philips PW3040 diffractometer with Cu K radiation (2 range = 20°-80°; step = 0.05 ° 2; time per step = 0.2 s).

3.6. Design of Experiment

Using design-expert software, the RSM research was carried out (Stat-Ease, Inc. Version 11.0) using the Central Composite Design (CCD). Adsorbent dose (A), pH (B), concentration (C), agitation speed (D), and dosage were the variables that were coded. The feasibility of the model equation was assessed utilizing a significant method of analysis of variance at a level of 5% significance (ANOVA) like other studies [9,18,19]. Equation (1) was used to approximate the relationship between response and independent variables.

$$Y = \beta_0 + \sum_{i=1}^k \beta_j x_j + \sum_{i=1}^k \beta_{jj} x_{ii} + \sum_{1 \leq i < j \leq k} \beta_{ij} x_i x_j \quad (9)$$

Where, Y denotes the response, k denotes number of applied variables, β₀ denotes intercept of the coefficient, β_i denotes linear terms applied, β_{jj} denotes squared coefficients of the applied terms, β_{ij} denotes interaction the coefficients terms, x_i and x_j are the coded independent variables applied for the study.

4. Conclusion

The environmental problems caused by the discharge of dyes (MB) from textile industries into water bodies could be addressed by the utilization of JHC. In this study, the JHC was carbonized and activated with ZnCl₂ to improve the adsorptive capacity. Analysis of the isotherm models shows that the experimental findings can be best illustrated by the Freundlich isotherm model, and the Pseudo-Second Order model clarified the adsorption kinetic results well. The ANOVA result showed that operational parameters are influential in the adsorption process. The JHC adsorbent is a regenerable, environmentally friendly, effective, and low-cost biomaterial for application in the removal of MB from aqueous dye solutions and industrial effluents.

References

- [1] K. Karthick, C. Namasivayam, and L. A. Pragasan, Utilization of ZnCl₂ activated Jatropha husk carbon for the removal of reactive and basic dyes: Adsorption equilibrium and kinetic studies, *Sus. Env. Resrch.*, 24 (2014) 139–148.
- [2] K. Karthick, C. Namasivayam, and L. A. Pragasan, Kinetics and isotherm studies on acid dye adsorption using thermal and chemical activated jatropha husk carbons, *Env. Prog. Sus. Eng.*, 37 (2018) 719–732.
- [3] I. J. Idan, S. N. Jamil, L. C. Abdullah, Removal of reactive anionic dyes from binary solutions by adsorption onto quaternized kenaf core fiber, *Int. J. Chem. Eng.*, 4 (2017) 1–13.
- [4] Y. P. Musa, and Z. A. Zurina, A sustainable and eco-friendly technique for dye adsorption from aqueous media using waste from Jatropha curcas (isotherm and kinetic model), *Desal. Wat. Treat.*, 182 (2020) 365–374.
- [5] S. Charola, H. Patel, and S. Chandna, Optimization to

- prepare porous carbon from mustard husk using response surface methodology adopted with central composite design, *J. Clnr. Prod.*, 223 (2019) 969–979.
- [6] H. D. Setiabudi, R. Jusoh, and S. F. Suhaimi, Adsorption of methylene blue onto oil palm (*Elaeis guineensis*) leaves: Process optimization, isotherm, kinetics and thermodynamic studies, *J. Tai. Inst. Chem. Eng.*, 63 (2016) 363–370.
- [7] A. Samimi, K. Kavosi, S. Zarinabadi, A. Bozorgian, Optimization of the Gasoline Production Plant in order to Increase Feed, *Prog. Chem. Biochem. Res.*, 3 (2020), 7–19.
- [8] S. Liu, J. Li, and S. Xu, A modified method for enhancing adsorption capability of banana pseudostem biochar towards methylene blue at low temperature, *Biores. Techn.*, 282 (2019) 48–55.
- [9] E. Vunain, and T. Biswick, Adsorptive removal of methylene blue from aqueous solution on activated carbon prepared from Malawian baobab fruit shell wastes: Equilibrium, kinetics and thermodynamic studies, *Sep. Sci. Tech.*, 54 (2019) 27–41.
- [11] A. P. Rawat, V. Kumar, and D. P. Singh, A combined effect of adsorption and reduction potential of biochar derived from Mentha plant waste on removal of methylene blue dye from aqueous solution, *Sep. Scie. Tech.*, 35 (2019) 1–15.
- [12] P. Sathishkumar, A. Mand, and T. Palvannan, Utilization of agro-industrial waste jatropha curcas pods as an activated carbon for the adsorption of reactive dye Remazol Brilliant Blue R (RBBR), *J. Clean. Prod.*, 22 (2012) 67–75.
- [13] P. Senthil, S. J. Varjani, and S. Suganya, Treatment of dye wastewater using an ultrasonic aided nanoparticle stacked activated carbon: Kinetic and isotherm modelling, *Bio. Tech.*, 250 (2018) 716–722.
- [14] A. Bozorgian, Z. Arab Aboosadi, A. Mohammadi, B. Honarvar, A. Azimi, Optimization of determination of CO₂ gas hydrates surface tension in the presence of non-ionic surfactants and TBAC, *Eurasian Chem. Commun.*, 2 (2020), 420–426.
- [15] B. Mella, J. Benvenuti, R. F. Oliveira, Preparation and characterization of activated carbon produced from tannery solid waste applied for tannery wastewater treatment, *Env. Sci. Pol. Res.*, 26 (2019) 6811–6817.
- [16] K. Karthick, C. Namasivayam, and L. A. Pragasan, Removal of direct red 12B from aqueous medium by ZnCl₂ activated jatropha husk carbon: Adsorption dynamics and equilibrium studies, *Ind. J. Chem. Tech.*, 24 (2017) 73–81.
- [17] Y. P. Musa, Z. A. Zurina, and A. R. Suraya, Eco-friendly sustainable fluorescent carbon dots for the adsorption of heavy metal ions in aqueous environment, *Nanomaterials*, 10 (2020) 315–331.
- [17] Z. Z. Abidin, N. Madehi, and R. Yunus, Coagulative behaviour of *jatropha curcas* and its performance in wastewater treatment, *Env. Prog. Sus. Eng.* 36 (2017) 1709–1718.
- [18] K. Silas, W. A. W. Ghani, T. S. Y. Choong, and U. Rashid, Optimization of activated carbon monolith Co₃O₄-based catalyst for simultaneous SO₂/NO_x removal from flue gas using response surface methodology, *Combt. Sci. Tech.*, 56 (2019) 1–18.
- [19] A. Samimi, S. Zarinabadi, A. Bozorgian, Optimization of Corrosion Information in Oil and Gas Wells Using Electrochemical Experiments, *Int. J. New Chem.*, 8 (2021), 149–163..
- [20] S. Mohebali, D. Bastani, and H. Shayesteh, Methylene blue removal using modified celery (*Apium graveolens*) as a low-cost biosorbent in batch mode: Kinetic, equilibrium, and thermodynamic studies, *J. Mole. Str.*, 1173 (2018) 541–551.
- [21] Y. P. Teoh, M. A. Khan, and T. S. Y. Choong, Kinetic and isotherm studies for lead adsorption from aqueous phase on carbon coated monolith, *Chem. Eng. J.*, 217 (2013) 248–255.
- [22] A. Bozorgian, Investigation of the effect of Zinc Oxide Nano-particles and Cationic Surfactants on Carbon Dioxide Storage capacity, *Advanced Journal of Chemistry, Section B: Natural Products and Medical Chemistry*, 3 (2021), 54–61.
- [23] H. Ebadiolahzadeh, and Z. Mohammad, Competitive adsorption of methylene blue and Pb (II) ions on the nano-magnetic activated carbon and alumina, *Mat. Chem. Phy.*, 248 (2020) 122893–122902
- [24] K. Silas, W. A. W. Ghani, T. S. Y. Choong, and U. Rashid, Activated carbon monolith Co₃O₄based catalyst: Synthesis, characterization and adsorption studies, *Env. Tech. Innn.*, 1 (2018a) 273–285.
- [25] K. Silas, W. A. W. Ghani, T. S. Y. Choong, and U. Rashid, Breakthrough studies of Co₃O₄ supported activated carbon monolith for simultaneous SO₂/NO_x removal from flue gas, *Fuel Proc. Tech.*, 180 (2018b) 155–165.
- [26] K. A. Shroff, and V. K. Vaidya, Kinetics and equilibrium studies on biosorption of nickel from aqueous solution by dead fungal biomass of mucor hiemalis, *Chem. Eng. J.*, 171 (2011) 1234–1245.
- [27] A. Abdedayem, M. Guiza, and A. Ouederni, Copper supported on porous activated carbon obtained by wetness impregnation: Effect of preparation conditions on the ozonation catalyst's characteristics. *Com. Ren. Chim.*, 18 (2015) 100–109.
- [28] M. Bagheri Sadr, A. Bozorgian, An Overview of Gas Overflow in Gaseous Hydrates, *J. Chem. Rev.*, 3 (2021), 66–82
- [29] A. Bozorgian, Z. A. Aboosadi, A. Mohammadi, B. Honarvar, and A. Azimi, A, Evaluation of the effect of nonionic surfactants and TBAC on surface tension of CO₂ gas hydrate. *J Chem. Petr. Eng.* 54 (2020), 73–81.